Journal of the Optical Society of Korea, Vol. 7, No. 4, December 2003, pp. 269-274

Gaussian Apodization Technique in Holographic Demultiplexer Based on Photopolymer

Duc-Dung Do, Jun-Won An*, and Nam Kim

Dept. of Computer & Communication Eng., Chungbuk Nat'l Univ., Cheongju 361-763, KOREA
Research Institute for Computer & Information Communication, Cheongju 361-763, KOREA

Kwon-Yeon Lee

Dept. of Electronic Eng., Sunchon Nat'l Univ., Sunchon 540-742, KOREA

(Received June 23, 2003)

In this paper, a Gaussian apodization technique applied to a transmission volume hologram for holographic demultiplexer is proposed. The Gaussian apodized grating of 15 mm × 11 mm size, 38 μm thickness and 3.2 mm horizontal standard deviation of the Gaussian index modulation profile was fabricated. A 22-channel demultiplexer based on that grating has been optically demonstrated. The channel spacing, the interchannel cross-talk level and the channel uniformity of 0.8 nm, -30 dB and 1.5 dB, respectively, were obtained.

OCIS codes : 090.1970, 220.1230, 230.0250, 130.1750.

I. INTRODUCTION

In recent years, there have been some advances in research on dense wavelength division multiplexing (DWDM) systems. In a DWDM system, an optical demultiplexer plays a key role. Its main function is to receive from a fiber a beam consisting of multiple optical wavelengths and separate it into its frequency components, which are coupled in individual fibers, one for each frequency [1]. When the number of channels in a given wavelength range increases or channel spacing is narrower (0.4 nm), the interchannel cross-talk, which limits the high performance of a whole system, is more important. According to the International Telecommunication Union-Telecommunication Standardization Sector (ITU-T) recommendations, the interchannel cross-talk level should be smaller than -30 dB.

Now there are several different devices which can be used as optical demultiplexers. Those are dielectric thin film filters (TFFs), arrayed waveguide gratings (AWGs), fiber Bragg gratings (FBG) and diffraction gratings. Recently, a holographic demultiplexer based on a photopolymer volume grating that diffracts all optical channels into a single order and separates them among their wavelengths has been proposed [2]. It is possible to get high diffraction efficiency due to the volume phase nature of the grating. However, in this device, the cross-talk among channels is still high and does not satisfy the ITU-T recommendations. To realize a optical demultiplexer based on this scheme, it is necessary to improve the interchannel cross-talk parameter.

In other research fields, such as FBG and holographic memory based on crystals, there have been some attempts to suppress the side lobes of the output spectrum [3,4]. In these cases, the apodization technique, which the modulating amplitude is varied along the fiber axis or optical axis, was used. This method provides a great solution to reduce the cross-talk level through narrowing wavelength selectivity, as well as angular selectivity of these devices.

In this paper, we present an apodization method that is for the first time applied to a transmission volume hologram to reduce the interchannel cross-talk level in the volume holographic demultiplexer. We first summarize the basic theory of apodization to analyze the capability of using it in the demultiplexing scheme. This is followed by the presentation of the fabrication technique. The diffraction profiles are then characterized. The spectra are finally presented to show the great side-lobe suppression of the apodized grating compared with a uniform one.

II. THEORY

In order to separate different spectral DWDM channels, it is convenient to use the spatial filtering mechanism inherent to any diffraction grating. A polychromatic plane beam of multi wavelengths λ_n, where n is an index from 1 to the total number of wavelengths, is incident on an un-slanted transmission volume grating at angle θ_i which is defined in Fig. 1. The desired diffraction angle θ_{on} with respect to wavelength λ_n satisfying the constructive interference condition [5] is given by

$$\Lambda_g(\sin\theta_i + \sin\theta_{on}) = \lambda_n \tag{1}$$

where Λ_g is the grating period. For the volume grating, the highest diffraction efficiency is obtained when Bragg's condition is satisfied, that is $\theta_i = \theta_{on}$.

Therefore, the light dispersion due to wavelength detuning $\Delta\lambda$ is simply derived from Eq. (1), which gives

$$\Delta\theta = \frac{\Delta\lambda}{\Lambda_g \cos\theta_{on}} \tag{2}$$

Thus, for a given wavelength detuning, or a channel spacing, and for a fixed configuration, the grating period decides the amount of dispersion of diffracted beam in the incident plane.

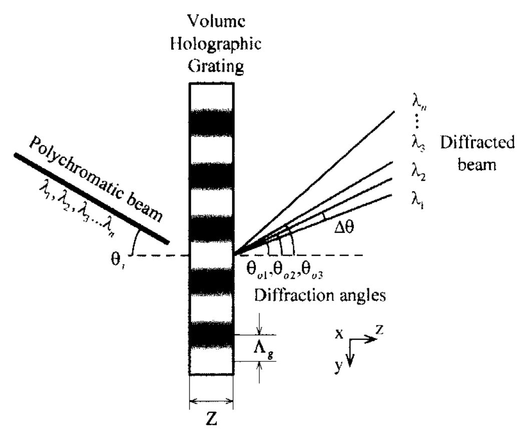

FIG. 1. Dispersion of multi-wavelengths by a transmission volume grating.

A volume grating in practice always has a finite size confined spatially by the recording medium. To understand the consequences of the finite grating size, three-dimensional Fourier analysis is used. Assuming that a volume phase grating has a local refractive index described as follows [6]

$$g(\vec{r}) = [1 + m\cos(\vec{K_g}\cdot\vec{r} + \phi_0)]\mathrm{rect}\frac{x}{X}\mathrm{rect}\frac{y}{Y}\mathrm{rect}\frac{z}{Z} \tag{3}$$

where $\vec{K_g}$ is the grating vector, $K_g = 2\pi/\Lambda_g$, ϕ_0 is an unimportant spatial phase of the grating, m is the modulation of the grating, $\vec{r}$ is the position vector with components (x, y, z) and X, Y, Z are the size of the grating in three rectangular coordinate directions.

The grating-vector spectrum of the above spatially bounded fringe is easily found to be [6]

$$G(\vec{K}) = \left[\delta(\vec{K}) + \frac{1}{2}\delta(\vec{K} - \vec{K_g}) + \frac{1}{2}\delta(\vec{K} + \vec{K_g})\right] \oplus XYZ\ \mathrm{sinc}\frac{Xk_X}{2\pi}\mathrm{sinc}\frac{Yk_Y}{2\pi}\mathrm{sinc}\frac{Zk_Z}{2\pi} \tag{4}$$

where k_X, k_Y, k_Z are the components of the spectral grating vector $\vec{K}$ projected on the x, y, z axes, respectively. From Eq. (4), it is obvious that a finite-size grating can be regarded as a superposition of a multitude of infinite-size gratings, each having a different K vector and a respective amplitude that is the coefficient of the Fourier transformation. The result of the convolution is a blurring of the grating-vector tip into a continuum of grating vectors surrounding the ideal location of the tip of the grating vector for an infinite grating. This blurring operation then leads to the possibility that the k-vector triangle required by the Bragg effect can be closed in many different ways, perhaps at some cost in terms of the strength of the diffracted wave.

From the Eq. (4), it is seen that in one dimension, the width of grating-vector spectrum is large as its respective size is small and vice versa. For the case of transmission gratings based on photopolymer, the material is very much thinner than their lateral extent. Therefore, the grating-vector cloud is extended in the direction normal to the recording surface. This geometry is quite tolerant to changes of the wavelength of the input beam, as shown in Fig. 2(a). In other words, transmission gratings have a wide wavelength selectivity that was approximately determined [7] by

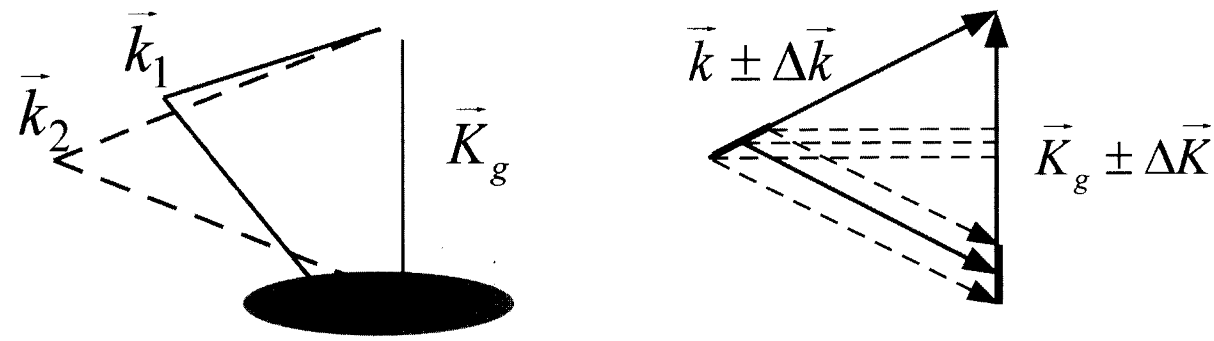

(a) (b)

FIG. 2. a) Grating-vector clouds and their effect on closing the k-vector triangle. b) Vector diagram of a bandwidth of a channel.

$$\frac{\Delta\lambda}{\lambda} = \frac{\Lambda_g}{Z}\cot\theta \tag{5}$$

where θ is an incident angle inside the material.

It is consequently seen that a thinner grating, as long as it is considered to be a volume one, will support more channels for a given channel spacing. Because the output beam is just diffracted along this horizontal direction, the effect of finite grating size on only the y-axis will be dealt with. As shown in Fig. 2(b), there is not only a grating vector $\vec{K_g}$ but also other extending ones that combine with the light of different wavelengths existing in the input beam to satisfy Bragg's condition. The light of different wavelengths that diffracted in the same direction makes up the bandwidth of an output channel and the inter-channel cross-talk. In the cases of holographic memory or demultiplexing schemes using multi gratings, this bandwidth and cross-talk are much smaller than those made by the wavelength selectivity and angular selectivity, so they are often ignored. Nevertheless, in our scheme, supported channels are contained in the range of the wavelength selectivity and are overlapped by each other due to the effect of finite extent grating size. When the channel spacing is reduced, this overlap is the important point.

Quantitatively, it is pointed out by H. Kogelnik in the coupled wave theory [7] that the diffraction efficiency of the diffraction beam for an un-slanted lossless dielectric transmission grating is as follows

$$\eta = \frac{\sin^2\sqrt{\xi^2+\nu^2}}{1+\xi^2/\nu^2}; \quad \nu = \frac{\pi G(\vec{K})Z}{\lambda_n\cos\theta}; \quad \xi = \frac{\Gamma Z}{2\cos\theta} \tag{6}$$

When the mismatch Γ to the Bragg's condition is very small, the spectrum of a channel is closely similar to the sinc^2 function. It is evident that the side lobes of the spectrum are large. These lead to a high cross-talk level between the adjacent channels. If the uniform function of the modulating amplitude is replaced by one that vanishes smoothly at the edges of the grating, the slowly decaying side lobes of the sinc^2 curve are eliminated, i.e. the cross-talk will be significantly reduced.

In this paper, a Gaussian function is chosen as an apodization profile because a Gaussian intensity distribution of laser beam can be obtained easily by a laser source. If the refractive index profile for a grating modulated in the y direction is given by

$$n(y) = n_0 + \Delta n(y)\cos(K_g \cdot y) \tag{7}$$

$$\text{and} \quad \Delta n(y) = \Delta n_0 \exp\left(-\frac{y^2}{2\sigma^2}\right) \tag{8}$$

where n_0 is the average refractive index of the holographic material, Δn_0 is the peak index modulation, the grating-vector spectrum is obtained to be

$$G(\vec{K}) = \left[\delta(\vec{K}) + \frac{1}{2}\delta(\vec{K}-\vec{K_g}) + \frac{1}{2}\delta(\vec{K}+\vec{K_g})\right] \oplus \Delta n_0 \exp\left(-\frac{\sigma^2 k_y^2}{2}\right) \oplus Y\text{sinc}\frac{Yk_Y}{2\pi} \tag{9}$$

Although the second convolution results in a wider main lobe, it also suppresses side lobes of the spectrum of the output channels. The amount of suppression depends on the ratio of the standard deviation σ to the size of the grating in the apodized direction. The output spectra can be simulated by using Eq. (4)

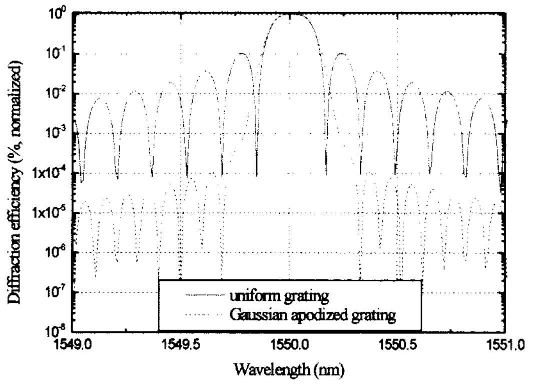

FIG. 3. Output spectral simulation for uniform and Gaussian apodized gratings.

and (9) to solve directly the differential equations of the coupled wave theory [7] for a uniform and Gaussian apodized grating, respectively. Fig. 3 shows the results of the simulation to compare the side-lobe suppression. The uniform grating has the horizontal size of 10 mm while that of the Gaussian grating is 16 mm. The standard deviation of the Gaussian profile is 3.2 mm. It is shown that both cases have same 3-dB bandwidth but the side-lobe suppression of 30 dB is achieved for the apodized grating.

III. FABRICATION OF GAUSSIAN APODIZED GRATING

According to the above analyses, a Gaussian apodized grating was fabricated on Du Pont's HRF-150-38 photopolymer. This 38-μm-thick photopolymer has a long shelf life, wide spectral sensitivity, volume phase holographic properties, and overall ease of use [8].

The optical system for recording and checking the grating is shown in Fig. 4. The Gaussian laser beam at 532 nm from a CW Nd-YAG source was expanded by a spatial filter and a lens. As mentioned above, the cross-talk is created in only one direction, so it is just required to have a grating of Gaussian-modulated distribution in the horizontal direction but uniform in others in order to improve the overall diffraction efficiency. Therefore, the expanded Gaussian beam was once more enlarged in the vertical direction by a couple of cylindrical lenses. A beam splitter divided such laser beam into two beams with the ratio of 1:1. The grating was created by exposing the photopolymer for around 135 s under the interference of these two beams, each of which had the intensity in the center of 3.0 mW/cm^2. Then, the grating was fixed by UV exposure before it could be used as a demultiplexer.

In our experiment, the half angle θ_w between the recording beams outside the material was 15° , thus, the grating period Λ_g of 1.028 μm was created. Accordingly, the incident angle θ_i at the center-wavelength of 1550 nm was 48.945°. In these conditions, the wavelength selectivity or the operating bandwidth obtained by Eq. (5) was 73.043 nm.

To check the profile of recorded gratings, we used the 633 nm He-Ne laser beam as a probe. After being created, the grating was horizontally shifted over the probe beam by using a linear stage. The measured data was collected automatically by a computer. When the probe beam reached the grating, it had to have a very small spot size to distinguish any fast variation of the modulating amplitude along the apodized direction. Therefore, a focused Gaussian beam was employed.

Fig. 5 shows the results of a Gaussian apodized grating of 16 mm width created and measured by the above fabricating process. A Gaussian function expressed by Eq. (8) was used to fit to the measured data. The peak of the modulation amplitude and the standard deviation were 0.0055 and 3.18 mm, respectively. Thus, the standard deviation of the modulation amplitude profile was approximated to 3.2 mm. The little mismatch between the fitting line and the experimental data is explained in that the intensity

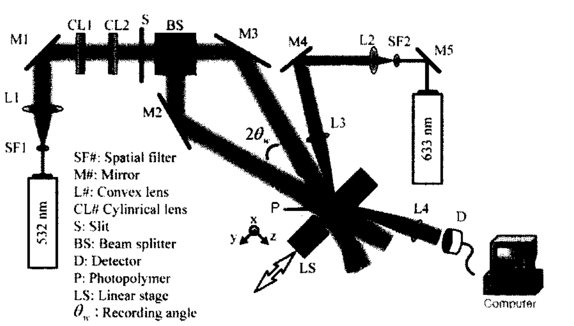

FIG. 4. Experimental system for recording and measuring grating.

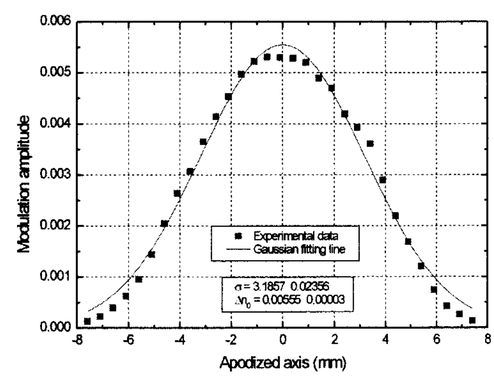

FIG. 5. Modulation amplitude as a function of position for an apodized grating.

response of the photopolymer is not linear at low recording intensity. This possibly affects the result of output spectral response. However, it would be overcome if another material of higher sensitivity were used.

IV. EXPERIMENTAL RESULTS

In this section, the experimental results of applying Gaussian apodization into a transmission volume grating for a holographic demultiplexer are presented. The structure of a demultiplexer consists of a collimating lens, a volume holographic grating, and an output lens, as shown in Fig. 6. The uniform light created by the collimating lens illuminates the grating and is diffracted at the angle of 48.945°. The output lens that has focal length F of 200 mm focuses channels into an output-fiber array. Nevertheless, for experimental convenience, in our configuration to measure the performance characteristics, instead of a fiber array we used only a single mode fiber that is moved along the focal plane and is controlled by a motorized fiber alignment unit. In addition, to demonstrate the high side-lobe suppression of the apodized grating, we have also made another uniform grating which has the same grating period as that of the Gaussian one. In the demultiplexer scheme, the diameter D of the readout beam was 6.5 mm for the uniform grating while it was 10.5 mm for the others.

Figs. 7(a) and (b) show the spectra of two output channels when using the uniform and the apodized grating, respectively. Each channel had 3-dB bandwidth of 0.18 nm and the channel spacing was 0.8 nm. These figures show the highly side-lobe suppression of about 20 dB consequently leading to the interchannel cross-talk reduction of 15 dB. However, the main-lobe

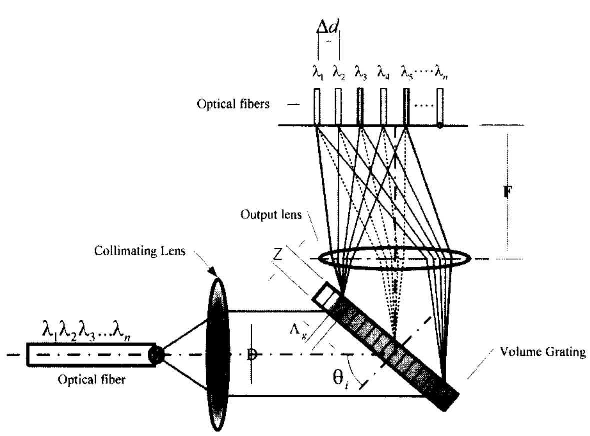

FIG. 6. Structure of a demultiplexer based on the photopolymer volume grating.

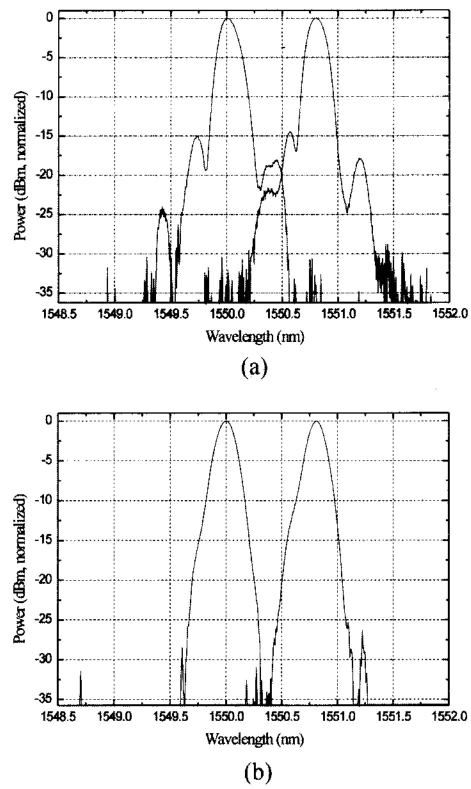

FIG. 7. The spectra of two output channels to compare the cross-talk reduction: a) Uniform grating, b) Gaussian apodized grating.

width of the spectral responses obtained experimentally was larger than that of the simulation results. It is obvious that the factor affecting our result must be the spot size of the focused beam because the Fraunhofer diffraction was not taken into account in the simulation, whereas the spot size of one channel in the experiment was about 47.7 μm. It is necessary to be matched with the fiber's core diameter to reduce the main-lobe width and increase the fiber-coupling efficiency. Therefore, other focal lengths of the output lens should be chosen properly to obtain better experimental data. Moreover, it was difficult to make the perfect uniform wave during the process of doing the experiment with the infrared light. This might also explain the difference of the main-lobe widths between theoretical and experimental results. Otherwise, coupling the light to the fiber also leads to asymmetric output spectra, as shown in Fig. 7. However, this effect is not much and can be eliminated if an exact experimental setup is carefully designed and constructed.

In our experiment, we have also tested the performance of the apodized grating working as a 22-channel demultiplexer. The channel characteristics have been

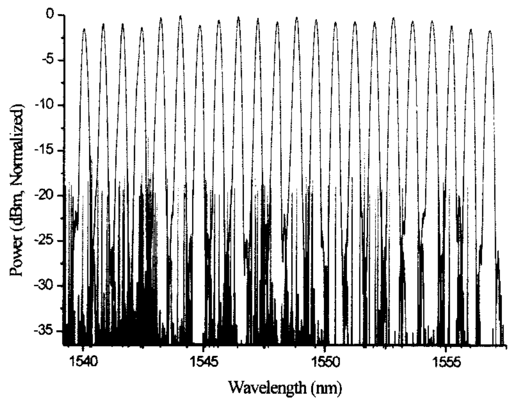

FIG. 8. Spectral response of 22-channel demultiplexer with 0.8 nm channel spacing.

measured in the flat region (1540-1557 nm) of the EDFA source to ensure the power uniformity over all test channels. The spectra of the output channels are shown in Fig. 8. The bandwidth of a channel was 0.18 nm. Two adjacent fibers were separated by 245-μm horizontal distance providing the wavelength spacing between each channel of 0.8 nm. Especially, the inter-channel cross-talk level was less than -30 dB. Besides, for all 22 channels, the interchannel uniformity of 1.5 dB was also obtained.

A drawback of applying the apodization technique to the transmission grating is an increase in the insertion loss because of its low diffraction efficiency at the outer parts. This partly rises from mismatching between the focused beam's spot size and the core diameter of output fiber. However, it can be improved when the readout beam size and focal length of the output lens are optimally selected. Commercially, to realize the demultiplexer based on volume apodized grating, the number of channels should be made higher by reducing the channel spacing to 0.4 nm or less. It is feasible and is currently being investigated more to reach that requirement.

V. CONCLUSIONS

In this paper, we have investigated the capability of applying apodization to the transmission grating for a demultiplexer in an optical communication system. This approach provides a high potential for suppressing the side lobes of the output spectra of a channel. By using the Gaussian function as the apodizing profile, we could reduce the cross-talk level of 0.8-nm-spaced channels down to -35 dB. In addition, we also have optically demonstrated a 22-channel demultiplexer of 1.5-dB interchannel uniformity, 0.8-nm channel spacing, and less than -30-dB interchannel cross-talk level.

As we have seen, the demultiplexer based on volume holographic apodized grating can perform better if we choose properly parameters such as a ratio of a standard deviation of a Gaussian function to a grating size that determines the readout beam side, and the output lens. By means of further researching on apodization technique, it is believed that the demultiplexer based on this scheme will be improved and realized to meet the needs of both existing and future DWDM systems.

*Corresponding author : Jwahn@osp.chungbuk.ac.kr.

REFERENCES

[1] S. V. Kartalopoulos, *Introduction to DWDM Technology*, pp. 89, SPIE press, 2000.

[2] J. W. An, N. Kim, and K. Y. Lee, "50 GHz-spaced 42-channel demultiplexer based on the photopolymer volume grating," *Jpn. J. Appl. Phys.*, vol. 41, no. 6B, pp. 665-666, 2002.

[3] T. Erdogan, "Fiber grating spectra," *J. of Lightwave Tech.*, vol. 15, no. 8, pp.1277-1294, 1997.

[4] D. Lande, S. S. Orlov, and L. Hesselink, "Two-photon apodization in lithium niobate," *Opt. Lett.*, vol. 23, no. 17, pp. 1399-1401, 1998.

[5] H. Smith, *Principles of holography*, (Wiley, New York, 1975), pp. 58.

[6] J. Goodman, *Introduction to Fourier Optics*,(McGraw-Hill, New York, 1996) Chap. 9, pp. 333-336, .

[7] H. Kogelnik, "Coupled wave theory for thick hologram gratings," *The Bell Sys. Tech. J.*, vol. 48, no. 9, pp. 2909-2947, 1969.

[8] U. S. Rhee, H. J. Caulfield, J. Shamir, C. S. Vikram, and M. M. Mirsalehi, "Characteristics of the Du Pont photopolymer for angularly multiplexed page-oriented holographic memories," *Opt. Eng.*, vol. 32, no. 8, pp. 1838-1847, 1993.

Journal of the Optical Society of Korea, Vol. 7, No. 4, December 2003, pp.275-278

CUMULATIVE AUTHOR INDEX

December 2003